

# X-ray diffraction imaging for predictive metrology of crack propagation in 450-mm diameter silicon wafers

B.K. Tanner,<sup>1,a)</sup> J. Wittge,<sup>2</sup> P. Vagovič,<sup>3</sup> T. Baumbach,<sup>3</sup> D. Allen,<sup>4</sup> P.J. McNally,<sup>4</sup> R. Bytheway,<sup>5</sup> D. Jacques,<sup>5</sup> M.C. Fossati,<sup>1</sup> D.K. Bowen,<sup>1</sup> J. Garagorri,<sup>6</sup> M.R. Elizalde,<sup>6</sup> and A.N. Danilewsky<sup>2</sup>

<sup>1</sup>Department of Physics, Durham University, South Road, Durham DH1 3LE, UK

<sup>2</sup>University of Freiburg, Kristallographie, Geowissenschaftliches Institut, Freiburg, Germany

<sup>3</sup>Karlsruhe Institute of Technology, Institut für Synchrotronstrahlung, Karlsruhe, Germany

<sup>4</sup>Dublin City University, School of Electronic Engineering, Dublin 9, Ireland

<sup>5</sup>Jordan Valley Semiconductors UK Ltd, Durham DH1 1TW, UK

<sup>6</sup>CEIT and Tecnun (University of Navarra), 20018 San Sebastián, Spain

(Received 6 February 2013; accepted 11 February 2013)

The apparatus for X-ray diffraction imaging (XRDI) of 450-mm wafers, is now placed at the ANKA synchrotron radiation source in Karlsruhe, is described in the context of the drive to inspect wafers for plastic deformation or mechanical damage. It is shown that full wafer maps at high resolution can be expected to take a few hours to record. However, we show from experiments on 200-, 300-, and 450-mm wafers that a perimeter-scan on a 450-mm wafer, to pick up edge damage and edge-originated slip sources, can be achieved in just over 10 min. Experiments at the Diamond Light Source, on wafers still in their cassettes, suggest that clean-room conditions may not be necessary for such characterization. We conclude that scaling up of the 300-mm format Jordan Valley tools, together with the existing facility at ANKA, provides satisfactory capability for future XRDI analysis of 450-mm wafers. © 2013 International Centre for Diffraction Data. [doi:10.1017/S0885715613000122]

Key words: X-ray diffraction imaging, synchrotron radiation, 450-mm Si wafer, crack propagation

## I. INTRODUCTION

For a number of years, the International SEMATECH Manufacturing Initiative (ISMI) has been coordinating developmental activities (Abell, 2008) aimed at building infrastructure to allow pilot-scale introduction of device fabrication on 450-mm silicon wafers by 2012. Despite comments from senior industry executives at Semicon West in 2009 that the move to 450-mm diameter wafers is “just a distraction”, in December 2010, Intel announced that it has plans to migrate production at its Oregon-based DX1 plant (Intel, 2010) to the 450-mm format. Its intention is to open the 22-nm node plant in 2013. Increase in wafer diameter will reduce manufacturing costs (Chien *et al.*, 2007; Jones, 2009) and increase output volume. However, there are significant material issues remaining and initially yield may fall on introduction of 450-mm wafer production.

Material issues associated with the use of 1 mm thick, 450-mm diameter wafers include planar chemical mechanical polishing at this diameter (Borucki *et al.*, 2009), plastic deformation associated with gravitational sag, and the increase in process and cooling times required. In addition, the increased weight poses an increased risk of mechanical damage at the edge of the wafer. As a part of the European Union funded SIDAM project, cracks introduced mechanically by misaligned handling tools have been identified as being responsible for fracture of 300-mm diameter wafers during high-temperature processing. We have used X-ray diffraction

imaging (XRDI; topography) (Bowen and Tanner, 2006) in both the laboratory and at the ANKA (Germany) and Diamond (UK) synchrotron radiation sources to record the images of cracks, similar to those produced by repeated collision of misaligned tools, generated by indentation at the bevel edge of 200-mm (8-inch) wafers. Using a semi-kinematic model of image formation, we have been able to identify those cracks that are likely to propagate and define a single critical parameter  $\kappa_c$  for their identification which can be directly determined from the X-ray images (Tanner *et al.*, 2012). The predictions from the measured  $\kappa$ -values have been shown to agree very well with experimental measurements of the probability of breakage of these wafers during rapid thermal annealing, using finite-element modeling to determine high-temperature thermal stresses.

Heavier wafers and larger handling tools are likely to result in a higher risk of fracture than on the existing fabrication lines. As the scale increases, the cost of halting the line to diagnose and remedy the faulty tool also increases. It is thus important that there exists a facility to study wafer damage and plastic deformation in 450-mm wafers. Extension of the capability of XRDI (Figure 1) for inspection of 450-mm wafers has been one of the objectives of the SIDAM program. Facilities are now in place at the ANKA synchrotron radiation source.

## II. SYNCHROTRON RADIATION XRDI

### A. 450-MM apparatus

Facilities for inspection of 300-mm silicon wafers by white radiation XRDI have been in place at the Topo-Tomo

<sup>a)</sup> Author to whom correspondence should be addressed. Electronic mail: b.k.tanner@dur.ac.uk

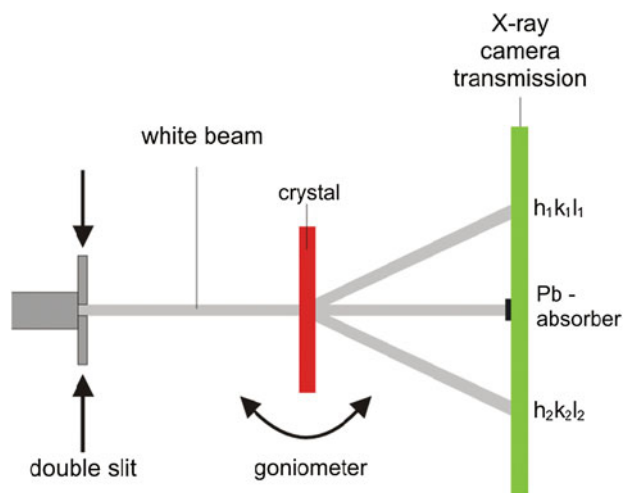


Figure 1. Principle of large area transmission topography at a synchrotron radiation source.

beamline (Simon and Danilewsky, 2003) of the ANKA synchrotron radiation source in Karlsruhe, Germany for some time (Danilwesky *et al.*, 2008a). The energy of the electrons inside the ANKA storage ring is 2.5 GeV which results in the characteristic wavelength of 2 Å. This is perfect for topography of inorganic materials and with a beam current of 200–100 mA, real-time imaging is possible using a CCD camera lens coupled to a thin phosphor screen (Rack *et al.*, 2008; Danilewsky *et al.*, 2008b). A special feature of the beamline is that there are no optical components between the source point from bending magnet and the experiment, except for one 0.5 mm thick, highly polished, Be-window directly in front of the experiment. The 30-m-long beamline and the small source result in high resolution of the topographs of about 1 μm.

The sample goniometer is mounted on linear slides and conversion from the 300-mm format (Danilewsky *et al.*, 2008a) to 450-mm capacity was straightforward. As there is plenty of space surrounding the goniometer, the additional capability (Figure 2) has been achieved by simply replacing the slides with the ones capable of 500-mm wafer travel in the X and Y directions, normal to the X-ray beam direction

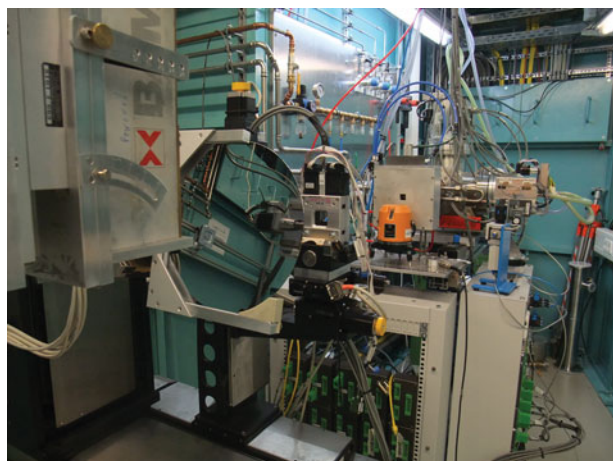


Figure 2. 300-mm wafer mounted in the goniometer and 500-mm translation stage.

(Z). Strain-free mounting of 200- and 300-mm diameter wafers has been successfully achieved by use of a grooved specimen holder with an adjustable clamp at one corner. The 450-mm sample holder is again only a scaled up version of the 300-mm wafer holder (Figure 3). Under strict commercial confidentiality conditions, we have successfully run 450-mm wafers using the translation stage and holder. There are no new experimental issues above those encountered in the inspection of 300-mm wafers and the data collection strategy described below proves satisfactory for 450-mm wafer inspection.

## B. Data collection strategy

A single shot inspection of large diameter silicon wafers at high resolution is clearly impossible and scanning of the sample is obviously a necessity. Furthermore, for rapid inspection, long integration times are unacceptable. An initial rapid survey is thus necessary, balancing resolution (and hence detection capability) with speed, followed by detailed inspection of identified defects (Danilewsky *et al.*, 2011). All instruments use charge coupled device (CCD) detectors coupled optically to a thin phosphor screen, enabling a variety of magnification strategies, either based on interchangeable lenses or fibre-optics, to be employed.

The design of the CCD detector at ANKA is based on the concepts of Hartmann *et al.* (1975) as well as Bonse and Busch (1996): the luminescence image of a scintillator screen is coupled via diffraction-limited visible light optics to a camera (CCD or CMOS). For our experiments, the microscope was equipped with a Rodenstock TV-Heliflex objective ( $f=50$  mm, max. NA=0.45), a Nikkor 180/2.8 ED ( $f=180$  mm) objective as tube lens, a pco.4000 CCD camera (4008 × 2672 pixels, 9 μm in size) and a 25 mm × 25 mm CdWO<sub>4</sub> (CWO) or Ce-doped Lu<sub>3</sub>Al<sub>5</sub>O<sub>12</sub> (LuAG) both polished scintillator single crystals, 300-μm-thick [3.6 × magnification, 2.5-μm effective pixel size, spatial resolution  $R > 5$  μm, 10.0 mm × 6.7 mm field of view (Nagornaya *et al.*, 2005; Rack *et al.*, 2009)]. The high stopping power of the CWO crystal in combination with light collection efficiency

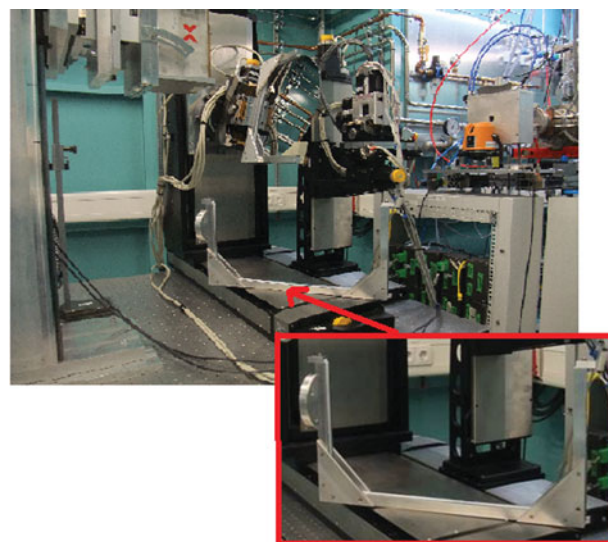


Figure 3. 500-mm stage and 300-mm wafer holder with wafer mounted. Inset: 450-mm wafer holder.

of the Rodenstock objective permits live imaging as already demonstrated for cineradiography with up to 250 images/s of living insects at Topo-Tomo (Betz *et al.*, 2008). Here, the pco.4000 camera with a Kodak KAI-11000 interline transfer chip gives access to frame rates of up to 5 images/s in the full-frame mode (depending on the dynamic range). Higher frame rates of up to 40 frames per second are accessible when working with a region of interest.

The small size of the scintillating crystals compared to photographic film area of  $13 \times 18 \text{ cm}^2$  limits the field of view to one single topograph and e.g. the  $(0\bar{2}2)$  reflection in the case of Si, has to be chosen. Improved resolution and sensitivity allow continuous imaging at frequencies between 1 and 10 Hz, while maintaining adequate topographic resolution. This increase in speed of the camera integration time allows us now to achieve a nearly real-time metrology of large wafers with high-speed scanning of the wafer.

Figure 4 shows a topograph from a perimeter scan of a 200-mm wafer, performed at the ANKA Topo-Tomo beamline. The original dislocation-free wafer shows, after a 60 s plateau anneal, a high number of extended defects, originating mainly at the wafer edge similar to the wafer shown in Figure 5. After image processing and dark correction, a frame rate of 40 frames per second results in effective integration of eight frames. The clarity of the laser label in Figure 4 is a sign of the high resolution which is achieved with the 0.2-s exposure time. Dense slip bands originate directly from the notch and we note that single  $60^\circ$ -dislocations can be resolved in the lower single slip band, which is located some distance from the edge.

As the scan time for a perimeter scan of a 200-mm wafer was approximately 5 min, it was immediately projected that the time for a similar scan of a 450-mm wafer would be approximately 11 min, as was found in practice. The greater weight of a 450-mm wafer results in greater bowing in comparison to 300-mm wafers. This stronger bending results in a larger (continuous) deviation of the position of the  $(0\bar{2}2)$  diffracted beam during the mapping which must now be corrected by moving the camera during the scan in the

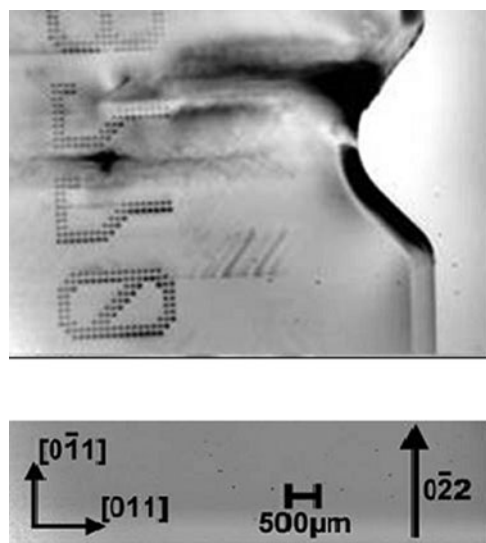


Figure 4. Metrology of 200-mm Si wafer *ex situ* at room temperature after 60 s plateau annealing at 1000 °C. Slip bands originate from the notch and laser written number.

direction parallel to the wafer. To enable this to be done automatically, we performed a calibration at four positions, rotated by  $90^\circ$ , close to the wafer edge at the beginning of the experiment from which the camera position correction was then calculated for every frame.

The ANKA facility therefore provides an acceptable European facility for characterization of 450-mm wafers by XRDI. At present, this cannot be achieved under clean-room conditions and significant investment would be required if these were to be set up. However, we have shown that for 200-mm wafers, high-quality and high-resolution XRDI can be performed on wafers in their cassettes (Figure 5). The critical energy of sources such as ANKA, Diamond, and the ESRF are such that transmission experiments on 1-mm thick wafers in cassettes are quite realistic. The exposure time penalty would be typically 20%.

### III. LABORATORY-BASED INSPECTION

The Jordan Valley BedeScan™ tool (Bowen *et al.*, 2003) was operated initially in the survey mode and subsequently in a high-resolution setting. In the survey mode, a CCD detector of pixel size  $23.5 \mu\text{m}$  and the adjacent three pixels were binned, giving an effective resolution of  $70.5 \mu\text{m}$ . The step size between each successive section topograph in the scan was six times the pixel size ( $141 \mu\text{m}$ ), giving a reasonable compromise between resolution and scan time. In the high-resolution mode, over a limited wafer area, a different CCD camera was used with an expanding fibre-optic faceplate, resulting in a pixel size of  $5 \mu\text{m}$ . There was no binning of pixels and the scan step was set at  $20 \mu\text{m}$  (four pixels). MoK $\alpha$  (wavelength 0.708 Å) radiation in the  $(022)$  reflection was used for the BedeScan™ images.

The examination of the full wafer map, taken with the BedeScan™ tool, of a 200-mm wafer that has been subjected to rapid thermal annealing (RTA) (Figure 6) reveals that after the heat treatment the original dislocation-free wafer shows a high number of dislocations and dense slip bands which arise from the wafer edge. From the notch (circled), it can be concluded that all the slip bands run parallel to  $\langle 110 \rangle$ , as is expected for the diamond structure type. The analysis of a

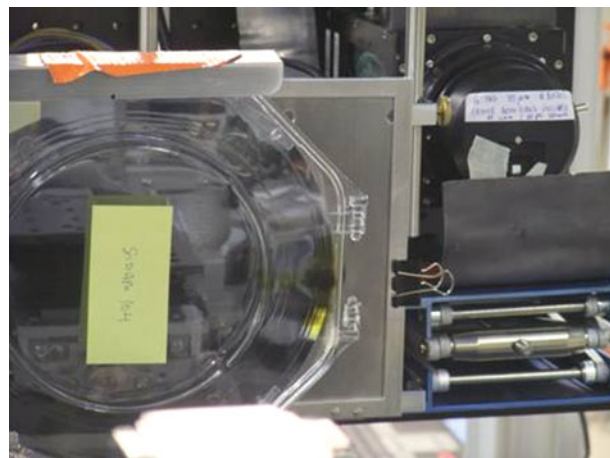


Figure 5. 200-mm wafer in its cassette mounted for white radiation XRDI at the Diamond Light Source. Note the radiation damage to the cassette as indicated by the red circle.



Figure 6. BedeScan™ transmission XRD Image of 200-mm plateau annealed Si wafer at 1000 °C for 30 s showing slip bands developing from the edge. Scan time 0.3 h.

number of wafer maps with different heating profiles shows that the length of a slip band is a function of the time the temperature stays above the brittle–ductile transition of Si at about 850–900 °C (Tanner *et al.*, 2011). The asymmetry associated with the slip band density, which is not predicted from the fourfold symmetry of the (001) wafer, has been shown to result from thermal anisotropy in the RTA furnace (Garagorri *et al.*, 2012). From the fast laboratory map, it is difficult to identify the origin of the slip bands; this could be done in high-resolution scans which were performed at the Topo-Tomo beamline of the ANKA synchrotron. However, we see from Figure 6 that the slip is usually initiated at the wafer edge and we have very few examples of the slip starting in the middle of the wafer. Furthermore, we have also determined that critical cracks resulting in wafer fracture originate at the wafer edge. Thus, an acceptable metrology is to undertake a perimeter scan, which can be done much more rapidly

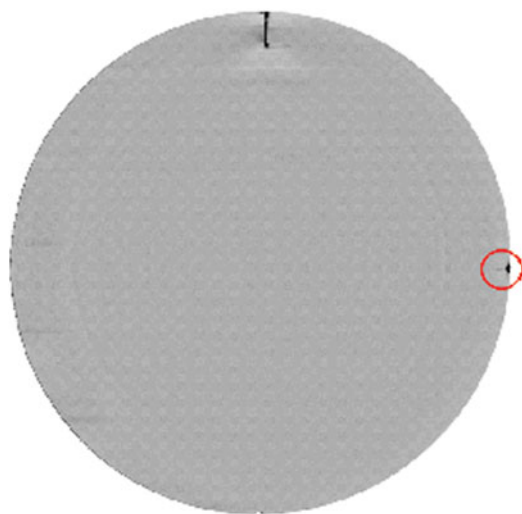


Figure 7. BedeScan™ transmission XRD Image of 200-mm (001) Si wafer which had been indented at 90, 180, and 270° with respect to the notch at the bottom of the image. The small crack circled on the right side is not visible optically.

TABLE I. Process time for complete wafer mapping at Topo-Tomo beamline, ANKA, (022) reflection, transmission mode, and in the laboratory on Jordan Valley BedeScan™, QCRT™, and QCTT™ instruments.

Diameter:	200 mm	300 mm	450 mm	450 mm <sup>a</sup>
ANKA beam size [mm <sup>2</sup> ]		5 × 5	4.5 × 7.5	5 × 8 <sup>a</sup>
Number of images		4700	7372	4000 <sup>a</sup>
Integration time [s]		0.5	0.5	0.1
Motor + Camera movement [s]		1.9	1.9	1.9
Total time [h]		3.1	5.0	2.2 <sup>a</sup>
BedeScan™ [h]	0.3	0.5	–	(1.1) <sup>b</sup>
QCRT™/QCTT™ [h]	0.16	0.25	–	(0.6) <sup>b</sup>

<sup>a</sup>Optimum performance, estimated from the actual experimental data in the previous columns. Minimum image overlap and integration time. Translation stage programmed to scan only the wafer area, eliminating blank frames.

<sup>b</sup>450-mm wafer capacity currently not available and time is estimated from experimental data in previous columns.

and in which the data collection time scales with wafer diameter, not area.

Figure 7 shows a full BedeScan™ image of a 200-mm diameter wafer that had been indented with a 50-N load on a Vickers tip at three points at 90, 180, and 270° with respect to the orientation notch, at the bottom of the image. When the indent was placed within about 70 μm of the bevel edge, long cracks were generated running toward the wafer centre. These appear with strong contrast in both BedeScan™ and synchrotron radiation topographs. In particular, the smaller crack, encircled in Figure 7, is not visible under an optical microscope, although it does appear in polarized infrared images. Such cracks, which result in catastrophic wafer fracture when heated to above 850 °C in an RTA furnace, are imaged in both transmission and reflection diffraction conditions, though the strongest contrast comes in transmission geometry.

#### IV. DATA COLLECTION TIMES

Table I indicates the time needed for complete mapping of wafers with different diameters at the ANKA Topo-Tomo beamline, compared with the laboratory BedeScan™, QCRT™, and QCTT™ tools running in a configuration optimized for speed. The ANKA data were taken using the digital camera system and the (022) reflection at 1-mm overlap between sequential images.

It is evident from Table I that full area maps of 300- and 450-mm wafers both at low resolution (BedeScan™/QCRT™/QCTT™) and at high resolution (ANKA) can be taken in a matter of hours.

#### V. CONCLUSION

Full high-resolution XRDI of 450-mm wafers has been performed in a few hours at the Topo-Tomo beamline on the ANKA storage ring. Experiments, using conventional source equipment on 200- and 300-mm wafers, indicate that full-wafer images of 450-mm wafers can be obtained in-fab, at low resolution, in less than an hour. Despite the significant size change imminent in the industry standard, XRDI of these very large wafers therefore remains possible both at synchrotron radiation sources and in the fab, though the latter does require apparently straightforward scaling up of present

300-mm tools. Facilities are thus in place to accommodate the extension of our studies of 200- and 300-mm wafer fracture to the 450-mm format when it becomes readily available. The application of our methodology for predicting the probability of catastrophic wafer breakage (Tanner *et al.*, 2012) during high-temperature processing will be appropriate for this new step in silicon wafer technology.

## ACKNOWLEDGEMENTS

This work was supported by the European Community Research Infrastructure Action under FP7 “Structuring the European Research Area” program. Financial support was provided through EU-FP7 project no. 216382 SIDAM. P.M.N. acknowledges additional support from Science Foundation Ireland’s Strategic Research Cluster Programme (“Precision” 08/SRC/I1411),

- Abell, T. (2008). “Realizing the 450 mm transition,” *Solid State Technol.* **51**, 22–30.
- Betz, O., Rack, A., Schmitt, C., Ershov, A., Dieterich, A., Körner, L., Ershov, A., and Baumbach, T. (2008). “High speed X-ray cineradiography for analyzing complex kinematics of living insects,” *Synchrotron Radiat. News* **21**, 34.
- Borucki, L., Philipossian, A., and Goldstein, M. (2009). “An analysis of potential 450 mm CMP tool scaling questions,” *Solid State Technol.* **52**, 10.
- Bonse, U., and Busch, F. (1996). “X-ray computed microtomography (mu CT) using synchrotron radiation (SR),” *Prog. Biophys. Mol. Biol.* **65**, 133–169.
- Bowen, D. K. and Tanner, B. K. (2006). *X-ray Metrology in Semiconductor Manufacturing* (CRC Taylor and Francis, Boca Raton).
- Bowen, D. K., Wormington, M., and Feichtinger, P. (2003). “A novel digital X-ray topography system,” *J. Phys. D* **36**, A17–23.
- Chien, C. F., Wang, J. K., Chang, T. C., and Wu, W. C. (2007). “Economic analysis of 450 mm wafer migration,” *Proc. Int. Symp. on Semiconductor Manufacturing*, p. 283–286.
- Danilewsky, A. N., Wittge, J., Rack, A., Weitkamp, T., Simon, R., Baumbach, T., and McNally, P. J. (2008a). “White beam topography of 300 mm Si wafers,” *J. Mater. Sci. – Mater. Electron.* **19**, S269–S272.
- Danilewsky, A. N., Rack, A., Wittge, J., Weitkamp, T., Simon, R., Riese-meier, H., and Baumbach, T. (2008b). “White beam synchrotron topography using a high resolution digital X-ray imaging detector,” *Nucl. Instrum. Methods Phys. B*, **266**, 2035–2040.
- Danilewsky, A. N., Wittge, J., Hess, A., Cröll, A., Rack, A., dos Santos Rolo, T., Allen, D., McNally, P., Vagovič, P., Li, Z., Baumbach, T., Gorostegui-Colinas, E., Garagorri, J., Elizalde, M. R., Jacques, D., Fossati, M. C., Bowen, D. K., and Tanner, B. K. (2011). “Real time X-ray diffraction imaging for semiconductor wafer metrology and high temperature *in-situ* experiments,” *Phys. Status Solidi a* **208**, 2499–2504.
- Garagorri, J., Elizalde, M. R., Fossati, M. C., Jacques, D., and Tanner, B. K. (2012). “Slip band distribution in rapid thermally annealed silicon wafers,” *J. Appl. Phys.* **111**, 094901.
- Hartmann, W., Markewitz, G., Rettenmaier, U., and Queisser, H. J. (1975). “High-resolution direct-display X-ray topography,” *Appl. Phys. Lett.* **27**, 308–309.
- Intel (2010). <http://www.bit-tech.net/news/hardware/2010/12/intel-plans-to-move-450mm-wafers>
- Jones, S. W. (2009). “300 mm Prime and the prospect for 450 mm wafers,” *Solid State Technol.* **52**, 14–15.
- Nagornaya, L., Onyshchenko, G., Pirogov, E., Starzhinskiy, N., Tupitsyna, I., Ryzhikov, V., Galich, Y., Vostretsov, Y., Galkin, S., and Voronkin, E. (2005). “Production of the high-quality CdWO<sub>4</sub> single crystals for application in CT and radiometric monitoring,” *Nucl. Instrum. Methods Phys. Res. A* **537**, 163–167.
- Rack, A., Zabler, S., Müller, B. R., Riese-meier, H., Weidemann, G., Lange, A., Goebels, J., Hentschel, M., and Görner, W. (2008). “High resolution synchrotron-based radiography and tomography using hard X-rays at the BAMline (BESSY II),” *Nucl. Instrum. Methods Phys. Res. A* **586**, 327–344.
- Rack, A., Weitkamp, T., Bauer Trabelsi, S., Modregger, P., Cecilia, A., dos Santos Rolo, T., Rack, T., Haas, D., Simon, R., Heldele, R., Schulz, M., Mayzel, B., Danilewsky, A. N., Waterstradt, T., Diets, W., Riese-meier, H., Müller, B. R., and Baumbach, T. (2009). “The micro-imaging station of the TopoTomo beamline at the ANKA synchrotron light source,” *Nucl. Instrum. Methods Phys. Res. B* **267**, 1978–1988.
- Simon, R. and Danilewsky, A. N. (2003). “The experimental station for white beam X-ray topography at the synchrotron light source ANKA, Karlsruhe,” *Nucl. Instrum. Methods Phys. B* **199**, 550–553.
- Tanner, B. K., Wittge, J., Allen, D., Fossati, M. C., Danilewsky, A. N., McNally, P., Garagorri, J., Elizalde, M. R., and Jacques, D. (2011). “Thermal slip sources at the extremity and bevel edge of silicon wafers,” *J. Appl. Cryst.* **44**, 489–494.
- Tanner, B. K., Fossati, M. C., Garagorri, J., Elizalde, M. R., Allen, D., McNally, P. J., Jacques, D., Wittge, J., and Danilewsky, A. N. (2012). “Prediction of the propagation probability of individual cracks in brittle single crystal materials,” *Appl. Phys. Lett.* **101**, 041903.